Vol 17 No 12, December 2008
1674-1056/2008/17(12)/4378-04

Chinese Physics B

© 2008 Chin. Phys. Soc.
and IOP Publishing Ltd

Quantization rules for low dimensional quantum dots

Xu Tian(许 田)[a)†], Cao Zhuang-Qi(曹庄琪)[b)], and Fang Jing-Huai(方靖淮)[a)]

[a)] *Physics department, Nantong University, Nantong 226001, China*

[b)] *Institute of Optics and Photonics, Shanghai Jiao Tong University, Shanghai 200240, China*

(Received 26 March 2008; revised manuscript received 14 April 2008)

This paper applies the analytical transfer matrix method (ATMM) to calculate energy eigenvalues of a particle in low dimensional sharp confining potential for the first time, and deduces the quantization rules of this system. It presents three cases in which the applied method works very well. In the first quantum dot, the energy eigenvalues and eigenfunction are obtained, and compared with those acquired from the exact numerical analysis and the WKB (Wentzel, Kramers and Brillouin) method; in the second or the third case, we get the energy eigenvalues by the ATMM, and compare them with the EBK (Einstein, Brillouin and Keller) results or the wavefunction outcomes. From the comparisons, we find that the semiclassical method (WKB, EBK or wavefunction) is inexact in such systems.

Keywords: analytical transfer matrix method, quantization rules, energy eigenvalues, confining potential

PACC: 0365S, 0365G, 0365N, 0365D

1. Introduction

The bound-state spectrum can be obtained by solving the Schrödinger equation. If the potential profile is smoothly compared with the particle wavelength, we can obtain the energy spectrum by the semiclassical WKB[1−4] (Wentzel, Kramers, and Brillouin) method, EBK[5] (Einstein, Brillouin, and Keller) method or wavefunction,[6,7] which is applied in many fields as a bridge between classical and quantum mechanics.

With the advances in submicron technology, we have realized nanostructures of many various shapes. Quantum dots are small devices containing a tiny droplet of free electrons. They are fabricated in semiconductor material and have typical dimensions from nanometres to a few microns. Their structures are relative to the confined potential. However, the sharp confining potential leads to the inexactness of the semiclassical method. In this paper, we extend analytical transfer matrix method (ATMM)[8−13] to calculate the energy eigenvalues in some steep potential profiles.

2. ATMM

Now let us consider a particle in a central force potential confined in a circular disc with radius r_0 or spherical quantum dot. The radial wavefunction satisfies the Schrödinger equation

$$-\frac{\hbar^2}{2m}\bigtriangledown^2\psi + V_{\text{eff}}(r)\psi = E\psi, \tag{1}$$

with

$$V_{\text{eff}}(r) = V(r) + V_1, \tag{2}$$

where $V_1 = \hbar^2(n_l^2 - 1/4)/2mr^2$ for two dimensional system, $V_1 = \hbar^2 n_l(n_l+1)/2mr^2$ for three dimensional system.

The wavefunction obeys the boundary conditions $\psi(0) = 0$, $\psi(r_0) = 0$. Henceforth, we let $\hbar = m = 1$ for simplicity.

In Fig.1, the region of space can be divided into three parts:

Part 1: $r_{\text{C}} \leqslant r < r_{t_1}$, where $E < V_{\text{eff}}(r)$;

Part 2: $r_{t_1} \leqslant r \leqslant r_{t_2}$, where $E > V_{\text{eff}}(r)$;

†E-mail: tianxu@gmail.com

Part 3: $r_{t_2} < r \leqslant r_{\rm D}$, where $E < V_{\rm eff}(r)$.

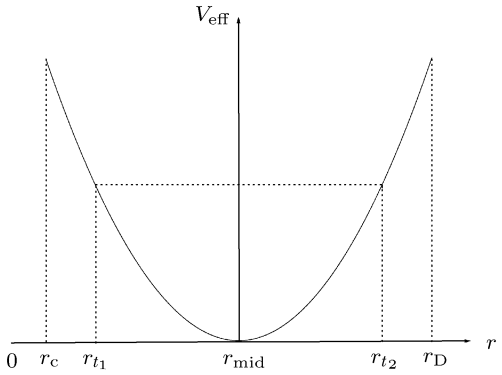


Fig.1. Sketch map of effective potential $V_{\rm eff}$ against r_0 when $r_0 > r_{t_2}$.

For explaining the problem easily, we move $V_{\rm eff}$ axis to the position $r_{\rm mid}$. r_{t_1} and r_{t_2} are the classical turning points; $r_{\rm C}$ and $r_{\rm D}$ are two points truncated by the confining wall and $r_{\rm C} \geq 0$. Three sections are divided into l, w and n section layers with equal width d respectively, and ATMM is applied to each region.

Defining $P = -\psi'(r)/\psi(r)$ and doing some algebraic calculation on the basis of Ref.[8], we obtain the following quantization condition when $r_0 > r_{t_2}$.

$$\int_{r_{t_1}}^{r_{t_2}} k{\rm d}r + \phi(s) = n_r\pi + \arctan\left(\frac{P_l}{k_{l+1}}\right) + \arctan\left(\frac{P_{l+w+1}}{k_{l+w}}\right), \quad n_r = 0, 1, 2, \ldots, \tag{3}$$

where $k = \sqrt{2m[E - V_{\rm eff}(r)]}/\hbar$, n_r is quantum number, $\arctan(P_l/k_{l+1})$ and $\arctan(P_{l+w+1}/k_{l+w})$ are the half phase shifts at the turning points. The phase contribution $\phi(s)$ for the reflections of sub-waves is written as[9]

$$\phi(s) = \int_{r_{t_1}}^{r_{t_2}} \left(-k'\frac{P}{P'}\right){\rm d}r. \tag{4}$$

When the half phase shifts are equal to $\pi/2$ at the turning points, Eq.(3) can be rewritten as

$$\int_{r_{t_1}}^{r_{t_2}} \left(k - k'\frac{P}{P'}\right){\rm d}r = (n_r + 1)\pi, \quad n_r = 0, 1, 2, \ldots. \tag{5}$$

If $r_{t_1} < r_0 < r_{t_2}$, the region of space is only divided into two segments, and the corresponding quantization rule is obtained by the same approach.

$$\int_{r_{t_1}}^{r_0} (k - k'\frac{P}{P'}){\rm d}r = \left(n_r + \frac{1}{2}\right)\pi. \quad n_r = 0, 1, 2, \ldots. \tag{6}$$

3. Applications

The quantization rules (Eqs.(5)–(6)) are applied to two simple central force confining potential: (1) the two-dimensional parabolic potential; (2) the spherical quantum dot.

3.1. The two-dimensional parabolic potential: $V(r) = r^2/2$

$r_{t_1} = \sqrt{E - \sqrt{E^2 - n_l^2 + 1/4}}$ and $r_{t_2} = \sqrt{E + \sqrt{E^2 - n_l^2 + 1/4}}$ are the classical turning points in this system. Using Eqs.(5) and (6), we get the energy eigenvalues in Table 1. When the energy has been determined, we can obtain the eigenfunctions $\psi(r)$ of the bound state in Fig.2 and an excited state in Fig.3 by the method in Ref.[11].

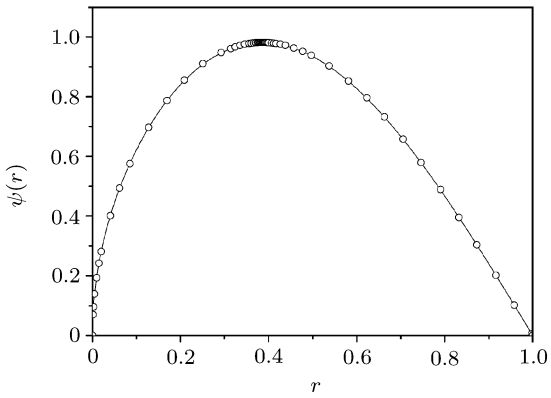


Fig.2. Plot of wavefunction $\psi(r)$ against r for the bound state of the two-dimensional harmonic oscillator. Solid line is obtained by the ATMM, while circles are obtained by the numerical technique. The confining radius is at $r_0 = 1.0$, $E = 3.0$.

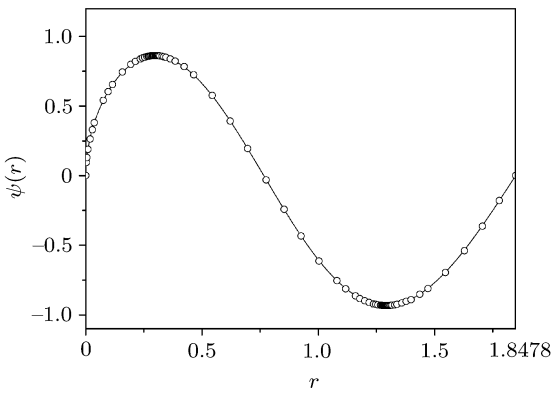


Fig.3. Plot of wavefunction $\psi(r)$ against r for an excited state of the two-dimensional harmonic oscillator. Solid curve is obtained by the ATMM, while circles are obtained by the numerical technique. The confining radius is at $r_0 = 1.8478$, $E = 5.0$.

From Table 1, we find that the WKB results show large deviation from the exact ones when r_0 is small. However, the ATMM results are equal to the exact ones.

Table 1. Energy eigenvalues obtained by the ATMM, the exact numerical method and the WKB approximation for the confined two-dimensional harmonic oscillator.

r_0	$E(n_r=1,n_l=0)$			$E(n_r=3,n_l=1)$		
	Exact	ATMM	WKB	Exact	ATMM	WKB
0.1	1523.6	1523.6	1509.8	8876.0	8876.0	8842.1
0.2	380.90	380.90	377.74	2219.0	2219.0	2214.5
0.3	169.30	169.30	167.94	986.24	986.24	984.58
0.5	60.981	60.981	60.493	355.08	355.08	354.55
1.0	15.392	15.392	15.280	88.927	88.927	88.800
1.5	7.1237	7.1237	7.0961	39.825	39.825	39.773
2.0	4.4405	4.4405	4.4699	22.860	22.860	22.837
2.5	3.4292	3.4292	3.5692	15.257	15.257	15.250

3.2. Spherical quantum dot

In this example, the classical trajectory of the electron is restricted between the hard-wall boundary at the surface and the centrifugal potential. It can be divided into two situations $n_l = 0$ and $n_l \neq 0$.

When $n_l = 0$, the radial Hamiltonian of the three-dimensional quantum dot is of one dimension, and we get the wavefunction

$$u_{n_r 0} = \sqrt{\frac{2}{r_0}} \sin \frac{(n_r+1)\pi r}{r_0}, \tag{7}$$

where r_0 is the radius of the dot. Then it is easier to obtain $\phi(s) = 0$ according to Eq.(4). We obtain the energy spectrum $E = \pi^2(n_r+1)^2/2r_0^2$, which is equal to the exact solution.

If $n_l \neq 0$, the turning point is $r_{t_1} = \sqrt{n_l(n_l+1)/(2E)}$. We apply the ATMM quantization rule Eq.(6) to this situation when $r_0/r_{t_1} \gg 1$, then get the same spectrum as the exact one which is shown in Table 2. The exact results are obtained by solving the spherical Bessel functions in Ref.[14]

In Ref.[5], the EBK method was used to obtain an approximate expression

$$E_{n_r,n_l} = \frac{\pi^2}{2mr_0^2}\left(n_r + \frac{3}{4} + \frac{\sqrt{n_l(n_l+1)}}{2}\right)^2. \tag{8}$$

In Table 2, the EBK results are acquired by using Eq.(8). We can find that the larger n_l, the larger deviations between the EBK results and the exact ones, whereas our method is exact.

Table 2. The ATMM energies compared with the exact and the EBK for the spherical quantum dot and $r_0 = 1$.

n_r	n_l	E_{Exact}	E_{ATMM}	E_{EBK}
0	2	16.612	16.612	19.244
1	2	41.360	41.360	43.669
0	3	24.416	24.416	30.401
1	3	54.257	54.257	59.833
2	3	93.818	93.818	99.134
0	4	33.481	33.481	43.995
1	4	68.504	68.504	78.408
0	5	43.767	43.767	60.059
1	5	84.072	84.072	99.425
0	6	55.262	55.262	78.577
1	6	100.919	100.919	122.895

3.3. The confined Hulthén potential

The Hulthén potential is usually used screened potential in physics. It has been used in many field such as in atomic physics[15,16] and in plasma physics.[17] So we are of great interest to investigate the properties of the system which consists of an ion and electron interacting through the Hulthén potential confined in a spherical box with radius r_0, and the ion is at the centre.[6]

In atomic units, the Hulthén potential can be written as

$$V(r) = \frac{-\delta \mathrm{e}^{-\delta r}}{1-\mathrm{e}^{-\delta r}}, \tag{9}$$

where δ is the screening parameter.

By Eqs.(5) and (6), energies are calculated for $1s$ and $2p$ state respectively. The results are shown in Tables 3 and 4 for different radius r_0, and two values of δ are considered. $E_{\rm exact}$ is calculated by numerical method, and $E_{\rm WF}$ is obtained by the wavefunction method. Comparison of the energy eigenvalues by ATMM with those by wavefunction reveals that the latter is inexact when r_0 is small, whereas ATMM has better accuracy.

Table 3. The ATMM energies for 1s state of the confined Hulthén potential compared with the exact results and the wavefunction ones for two values of the screening parameter. All energies are in Hartrees.

δ	r_0	$E_{\rm Exact}$	$E_{\rm ATMM}$	$E_{\rm WF}$
0.1	2.0	–0.07584	–0.07584	–0.07570
	2.5	–0.28583	–0.28583	–0.28576
	3.0	–0.37496	–0.37496	–0.37489
	4.0	–0.43440	–0.43440	–0.43421
	5.0	–0.44767	–0.44767	–0.44740
	6.0	–0.45053	–0.45053	–0.45035
	7.0	–0.45111	–0.45111	–0.45102
	8.0	–0.45122	–0.45122	–0.45118
	9.0	–0.45125	–0.45125	–0.45119
	10.0	–0.45125	–0.45125	–0.45124
0.2	2.0	–0.02800	–0.02800	–0.02784
	2.5	–0.23838	–0.23838	–0.23830
	3.0	–0.32784	–0.32784	–0.32777
	4.0	–0.38774	–0.38774	–0.38756
	5.0	–0.40127	–0.40127	–0.40099
	6.0	–0.40423	–0.40423	–0.40404
	7.0	–0.40485	–0.40485	–0.40476
	8.0	–0.40497	–0.40497	–0.40493
	9.0	–0.40499	–0.40499	–0.40498
	10.0	–0.40500	–0.40500	–0.40499

Table 4. The ATMM energies for 2p state of the confined Hulthén potential compared with the exact results and the wavefunction ones for two values of the screening parameter. All energies are in Hartrees.

δ	r_0	$E_{\rm Exact}$	$E_{\rm ATMM}$	$E_{\rm WF}$
0.1	6.0	–0.00815	–0.00815	–0.00812
	7.0	–0.04039	–0.04039	–0.04037
	8.0	–0.05764	–0.05764	–0.05762
	9.0	–0.06716	–0.06716	–0.06714
	10.0	–0.07250	–0.07250	–0.07247
	15.0	–0.07888	–0.07888	–0.07885
	20.0	–0.07917	–0.07917	–0.07916
0.2	8.0	–0.01710	–0.01710	–0.01709
	9.0	–0.02736	–0.02736	–0.02734
	10.0	–0.03330	–0.03330	–0.03329
	15.0	–0.04128	–0.04128	–0.04125
	20.0	–0.04185	–0.04185	–0.04181
	25.0	–0.04188	–0.04188	–0.04188
	30.0	–0.04189	–0.04189	–0.04188

4. Conclusions and discussion

This paper is the first attempt to extend ATMM to calculate the energy eigenvalues and wavefunctions of a particle confined in low dimensional sharp confining potentials. In these cases, ATMM works better than WKB method, EBK method or wavefunction, which are more or less deviated from the exact values. Why ATMM is exact? One reason is that the accurate phase shift at the turning points are acquired, the other is that the scattering of the sub-waves are taken into account. Two quantization rules Eqs.(5) and (6) obtained from our method give us an easy way to calculate the bound-state spectrum for both smooth and steep potentials.

References

[1] Sinha A, Roychoudhury R and Varshni Y P 2003 *Phys.* B **325** 214
[2] Friedrich H and Trost J 1999 *Phys. Rev.* A **59** 1683
[3] Hervé G 1996 *Chem. Phys. Lett.* **262** 759
[4] Barnali C and Tapan K 1999 *Phys. Rev.* A **60** 104
[5] Chen W 2003 *Phys. Rev.* B **68** 205104
[6] Varshni Y P 2004 *Modern Phys. Lett.* A **19** 2757
[7] Varshni Y P 1998 *J. Phys.* B **31** 2849
[8] Cao Z Q, Liu Q, Shen Q S, Dou X M and Chen Y L 2001 *Phys. Rev.* A **63** 054103
[9] Ou Y C and Cao Z Q 2004 *J. Chem. Phys.* **121** 16
[10] Xu T and Cao Z Q 2006 *Chin. Phys.* **15** 1172
[11] He Y, Cao Z Q and Shen Q S 2004 *Chin. Phys. Lett.* **21** 2089
[12] Cao Z Q, Jiang Y, Shen Q S, Dou X M and Chen Y L 1999 *J. Opt. Sci. Am.* A **16** 2209
[13] Zhou F, Cao Z Q and Shen Q S 2003 *Phys. Rev.* A **67** 062112
[14] Flügge S 1974 *Practical Quantum Mechanics* **162**
[15] Lam C S and Varshni Y P 1986 *Phys. Rev.* A **4** 1875
[16] Dutt R 1985 *J. Phys.* A **18** 379
[17] Yoon J H and Yun Y 2000 *Korean Phys. Soc.* **37** 73